Eur. Phys. J. C 51, 367–375 (2007)
DOI 10.1140/epjc/s10052-007-0283-x

THE EUROPEAN PHYSICAL JOURNAL C

Regular Article – Theoretical Physics

A quantum mechanical description of the experiment on the observation of gravitationally bound states

A. Westphal[1,a,b], H. Abele[1], S. Baeßler[2], V.V. Nesvizhevsky[3], K.V. Protasov[4], A.Y. Voronin[5]

[1] Physikalisches Institut der Universität Heidelberg, Philosophenweg 12, 69120 Heidelberg, Germany
[2] Institut für Physik, Universität Mainz, Staudinger Weg 7, 55128 Mainz, Germany
[3] Institut Laue langevin, 6 rue Jules Horowitz, 38042, Grenoble, France
[4] LPSC, IN2P3-CNRS, UJFG, 53, Avenue des Martyrs, 38026 Grenoble, France
[5] P.N. Lebedev Physical Institute, 53 Leninsky Prospekt, 119991, Moscow, Russia

Received: 20 February 2006 /
Published online: 12 June 2007 –

Abstract. Quantum states in the earth's gravitational field have been observed, with ultra-cold neutrons falling under gravity. The experimental results can be described by the quantum mechanical scattering model presented here. We also discuss other geometries of the experimental setup, which correspond to the absence or the reversion of gravity. Since our quantum mechanical model quantitatively describes, particularly, the experimentally realized situation of reversed gravity, we can practically rule out alternative explanations of the quantum states, in terms of pure confinement effects.

PACS. 03.65.Ge; 03.65.Ta; 04.62.+v; 04.80.-y; 61.12.Ex

1 Introduction

A gravitationally bound quantum system has been realized experimentally with ultra-cold neutrons falling under gravity and reflecting off a "neutron mirror" [1,2]. UCN are neutrons that, in contrast to faster neutrons, are reflected at all angles of incidence. For such UCN, flat surfaces thus act as mirrors. Using an efficient neutron absorber for the removal of higher unwanted states, only neutrons in selected energy states are taken. This idea of observing quantum effects occurring when ultra-cold neutrons are stored on a plane matter surface was first discussed by Lushikov and Frank [3] with the first concrete experimental realization in [4]. An experiment in some aspects similar was discussed by Wallis et al. [5] in the context of trapping atoms in a gravitational cavity. The toy model of a Schrödinger quantum particle bouncing in a linear gravitational field is known as the quantum bouncer [6,7]. Retroreflectors for atoms have used the electric dipole force in an evanescent light wave [8,9], or they are based on the gradient of the magnetic dipole interaction, which has the advantage of not requiring a laser [10].

A unique side-effect of the experiment with neutrons is its sensitivity to gravity-like forces at length scales below 10 μm, while all electromagnetic effects are extremely suppressed [11,12]. The quantum states probe Newtonian gravity between 10^{-9} and 10^{-5} m and the experiment places limits for gravity-like forces in this case. In light of recent theoretical developments in higher-dimensional field theory [13–16] (see also [17,18] for explicit realizations in string theory), gauge fields could mediate forces that are 10^6 to 10^{12} times stronger than gravity at submillimeter distances, exactly in the interesting range of this experiment, and they might give a signal in an improved setup.

In this article, we provide the details of a quantum mechanical calculation [19] for our experiment, where gravitationally bound quantum states are observed for the first time. The experiment consists of a reflector for neutrons, called a neutron mirror, a remover for unwanted neutrons, called an absorber and a neutron detector. In our previous papers [1,2,20] the experiment and a first treatment of the data were presented. Fundamental limits for the spatial resolution and a first ansatz to incorporate the neutron scatterer can be found in [20]. In another work [21] a description of the neutron loss from first principles was developed in which the rough edges of the absorber surface are treated as a time-dependent variation of a *flat* absorber position, modeling the neutron loss mechanism as a process equivalent to the ionization of a particle, initially confined in a well with an oscillating wall. Within the primary and simple model we present in this paper, we are able to describe the experimental data with one micro-physical fit parameter that parameterizes the micro-physics of the neutron scatterer/absorber. At the moment our model is the only one yet in which both the data in Figs. 2 and 4 are described.

[a] e-mail: westphal@sissa.it
[b] Present address: ISAS-SISSA and INFN, Via Beirut 2–4, 34014 Trieste, Italy

The setup of this paper is the following: after describing the experiment and the observations, we recall the quantum mechanics of gravitationally bound states on a free mirror that is without an absorber/scatterer. Then we present an approach to describe the state selection by deriving the neutron loss rate due to non-specular scattering from the rough surface of our absorber. This approach explains the non-classical dependence of the transmission of the mirror–absorber system as a function of the height l of the absorber above the mirror; see Figs. 1 and 2. We take into account the deformation of the bound state wave functions due to the matter bulk of the state selector and compare the full prediction with the actual data. We also show that the data are only understood when gravity is present.

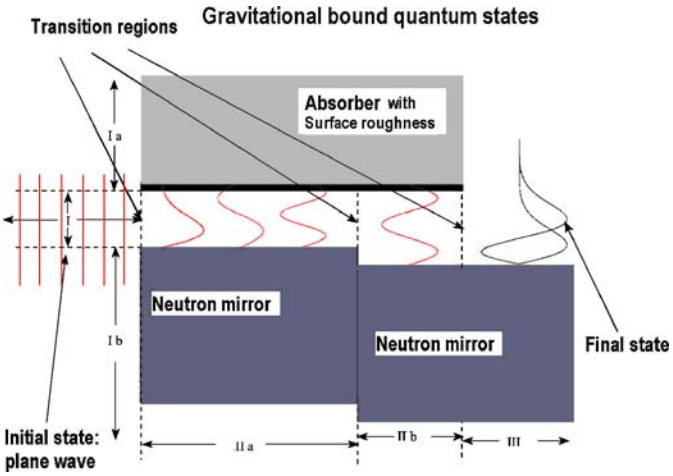

Fig. 1. Schematic view with mirrors, absorber and quantum mechanical boundary conditions. In the experiment, one mirror of length 10 cm or, as an option as shown here, two bottom mirrors of length 6 cm were used

2 Observation of quantum states and setup

A description of the experiment at the Institute Laue–Langevin (ILL) can be found in [2]. It was installed at the UCN facility PF2 of the Institute. Here, neutrons have a velocity of several meters per second. They are then guided to the experiment via a curved neutron guide with a diameter of 80 mm. At the entrance of the experiment, a collimation system cuts the energy down to an adjustable transversal energy $E_\perp$ in the pico-eV range. Either one solid block with dimensions 10 cm × 10 cm × 3 cm or two solid blocks with dimensions 10 cm × 6 cm × 3 cm composed of optical glass serve as mirrors for UCN neutron reflection. To select different states an absorber/scatterer, a rough mirror coated with an neutron absorbing alloy, is placed above the first mirror. We can vary the height l above the mirror, which is the size of the slit. The collimation system in front of the state selector is adjusted in such a way that neutrons on classical trajectories entering the experiment have to hit the mirror surface at least two times. After the second mirror we placed a ^{3}He counter for neutron detection. Figure 1 shows a schematic view of our setup. The signatures of the quantum states are observed in the following way: the ^{3}He counter measures the total neutron transmission F, when neutrons are traversing the mirror–absorber system as described. The transmission is measured as a function of the absorber height l and thus as a function of the energy of the neutron, since the height acts as a selector for the energy $E_\perp$ of the vertical motion. From the classical point of view, the transmission F of the

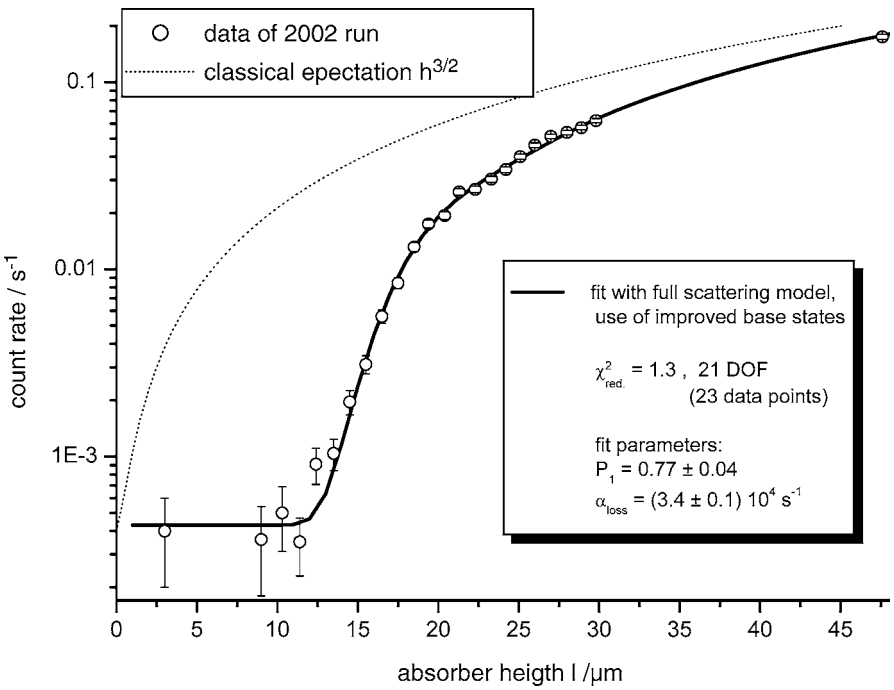

Fig. 2. *Circles*: data from the 2nd run 2002 with one bottom mirror [20]. *Solid*: transmission coefficient from the phenomenological scattering model. *Dash*: the classical expectation for the neutron transmission coefficient

neutrons is proportional to the phase space volume allowed by the absorber. It is governed by a power law: $F \sim l^n$ and $n = 3/2$.

The measurements show the following: Above an absorber/scatterer height of about 60 μm, the measured transmission is in agreement with the classical expectation but below 50 μm; a deviation is clearly visible. Below about 15 μm, no neutrons can pass the slit. In the next section we will find that the vertical extension of the gravitational bound states increases with the quantum number. Ideally, we expect a stepwise dependence of F as a function of l. If l is smaller than the spatial width of the lowest quantum state, then F will be zero. When l is equal to the spatial width of the lowest quantum state, F will increase sharply. A further increase in l should not increase F as long as l is smaller than the spatial width of the second quantum state. Then again, F should increase stepwise. At sufficiently high slit width one approaches the classical dependence. Figure 2 shows details of the quantum regime below an absorber height of $l = 50\,\mu$m. The transmission function depends on the horizontal neutron velocity and the absorption efficiency. It was found that, except for the ground state, the stepwise increase is mostly washed out.

3 Quantum mechanical description of gravitationally bound states

The quantum mechanical treatment of a reflecting neutron mirror, made from glass, is simple. The glass is described by a Fermi pseudo-potential $(V - \mathrm{i}W)$. This potential is essentially real ($|W| \ll |V|$), because of the small absorption cross section of glass and $V = 100$ neV is large compared with the transversal energy $E_\perp$ of the neutrons. Therefore, the potential V is set to infinity at height $z = 0$. Neutrons which hit the glass surface undergo specular reflections.

We start with the description of the free states. On a perfect mirror, no mixing of momentum components takes place, which leads to a decoupled one-dimensional stationary Schrödinger equation,

$$\left(-\frac{\hbar^2}{2m}\Delta + V(z)\right)\Psi_n = E_n\Psi_n,$$
$$V(z) = \begin{cases} mgz\,, & x \geq 0\,, \\ \infty\,, & x < 0\,, \end{cases} \qquad (1)$$

with the wave functions Ψ_n for the energies E_n and the potential $V(z)$. m is the mass of the neutron and g is the acceleration in the earth's gravitational field. It is convenient to use

$$\zeta = \frac{z}{R}$$

and, above the mirror,

$$V = mgR\zeta\,. \qquad (2)$$

Here, R is a scaling factor, defined by

$$R = \left(\frac{\hbar^2}{2m^2 g}\right)^{1/3}. \qquad (3)$$

The solutions $\Psi_{n,g}(\mathbf{r}, t)$ of (1) are obtained with an Airy function

$$\Psi_{n,g}(\mathbf{r}, t) = \phi(x, y)\psi_{n,g}(\zeta)\mathrm{e}^{-\mathrm{i}\frac{E_n}{\hbar}t},$$
$$\psi_{n,g}(\zeta) = \mathrm{Ai}(\zeta - \zeta_n)\,. \qquad (4)$$

The displacement ζ_n of the nth eigenfunction has to coincide with the nth zero of the Airy function ($\mathrm{Ai}(-\zeta_n) = 0$) to fulfill the boundary condition $\Psi_n(0)$=0 at the mirror. The corresponding energies E_n with $z_n = R\zeta_n$ are

$$E_n = mgz_n\,. \qquad (5)$$

In the WKB approximation we have to leading order

$$\zeta_n = \left(\frac{3}{2}\left(n - \frac{1}{4}\right)\right)^{2/3}, \qquad (6)$$

which coincides with the exact eigenvalues to better than 1 % even for the ground state [19]. The z_n correspond to the highest point of a classical neutron trajectory with energy E_n. For example, the energies of the lowest levels ($n = 1$, 2, 3, 4) are 1.44, 2.53, 3.42 and 4.21 peV. The corresponding classical turning points z_n are 13.7, 24.1, 32.5 and 40.1 μm.

The aim of this experiment was to populate only some of the lowest allowed gravitationally bound quantum states. Higher states were removed with the absorber/scatterer at a certain height l.

4 Phenomenological scattering model of neutron loss

It will be most convenient to start with a polychromatic neutron beam of (locally) plane waves entering the system. As is well known, gaussian wave packets being closer to the particle view of a neutron can easily be decomposed by a Fourier integral over plane waves. Using all boundary conditions given by Fig. 1, one arrives at a set of usual matching conditions [19]. The neutron transmission of the system depends both on the eigenvalues and the matching conditions. Furthermore, if two bottom mirrors are used optionally and shifted relative to each other by a few μm in height (as it was in the 1999 beam time), there is an additional boundary that changes the population of the eigenstates.

We find a system of linear equations for the matching constants, and its solution yields, finally, the transmission coefficient of the nth final bound state of region III. The initial population of the bound states of the wave guide system at coupling-out is uniform if the vertical velocity distribution of the arriving beam is sufficiently wide and flat – which is true in our case, where we have about 20 cm/s or 50 peV spread in the vertical components of the arriving

beam, to be compared to a few peV for the lowest vertically bound states inside the mirror–absorber system [12, 19].

In addition, we have to introduce repopulation coefficients p_j, which allow us to take into account an optional step between region IIa and IIb into account. If there is no step, all $p_j = 1$. In the 1999 beam time, the 2nd mirror has been shifted downwards by 5 μm relative to the 1st mirror. The matrix of the overlap integrals of the wave functions at the edge IIa/IIb is sufficiently diagonal, so that we can neglect the off-diagonal elements. We can set $p_1 = 0.25$ and $p_j = 1$ for $j > 1$. Hence, the relative shift of the bottom mirrors offers the possibility of controlling the relative population of in particular the ground state in the earth's gravitational field. However, even in the setup without step, we find a reduction of the ground state for unknown reasons and keep p_1 as a free parameter.

In the following, we take into account the absorber roughness as an additional loss channel in the one-dimensional Schrödinger equation. The neutron loss is then understood in terms of non-specular scattering of the neutrons into highly excited states, which due to their large vertical energy are rapidly lost inside the glass of the mirror and the absorber/scatterer. Scattering occurs at the rough and (due to $V_{\mathrm{absorber}} \simeq 10^{-8}\,\mathrm{eV} \gg E_n$ for states with low n) hard surface of the absorber, which notion shall enable us to derive the scattering-induced loss rate with just one undetermined micro-physical quantity. It can be given in a micro-physical scattering model as a function of the scattering cross section, but we prefer to consider it as a free parameter, which will be determined in the end by a fit to the data.

The deformation of the wave functions compared with the purely gravitationally bound states due to the large real part of the absorber potential leads to approximate vanishing of the bound states at the absorber surface. Therefore, the loss rate is calculated in terms of the deformed states.

The neutron removal processes are modeled as a general phenomenological loss rate $\Gamma_n(l)$ of the nth bound state, which is taken to be proportional to the probability density of the neutrons at the absorber/scatterer. Here l again denotes the position of the absorber/scatterer above the mirror. The modulus of the bound state is then no longer constant in time, since it is given as the solution at first order of a differential equation that determines the change of the norm to be proportional to its momentary value as well as the loss rate

$$\mathrm{d}\langle\psi_n|\psi_n\rangle = -\langle\psi_n|\psi_n\rangle\Gamma_n(l)\,\mathrm{d}t\,, \tag{7}$$

which yields

$$\langle\psi_n|\psi_n\rangle = |P_n(t)|^2, \quad P_n(t) = \mathrm{e}^{-\frac{1}{2}\Gamma_n(l)t}. \tag{8}$$

The roughness that causes the loss due to scattering can be thought of as being confined to a region of about 2σ width attached to an imagined absorber surface at a height l. Here σ denotes the rms height roughness of the absorber. Therefore, we give the loss rate of the nth bound state in terms of the general description of scattering processes as a function of the probability of neutrons to dwell within the roughness surface region of the absorber/scatterer as follows:

$$\Gamma_n(l) = \alpha_{\mathrm{loss},n} \int_{l-2\sigma}^{l} \mathrm{d}z|\psi_n(z)|^2. \tag{9}$$

Here we used the fact that the geometry of the wave guide system with and without gravity allows for coordinates (x, y, z) with z denoting the transverse coordinate for which the Schrödinger equation becomes separable with the product ansatz,

$$\phi_n(\mathbf{r}) = \psi_{n,g}(z)\phi_{xy}(x, y)$$

with

$$\phi_{xy}(x, y) = \frac{1}{\sqrt{A_{xy}}}\mathrm{e}^{\mathrm{i}k_x x + \mathrm{i}k_y y}. \tag{10}$$

Since losses due to non-specular scattering should only depend on local quantities of the surface and the probability of finding neutrons at this surface, we assume that the micro-physics of the neutron loss is independent of the 'macro'-physics of the wave function behavior. Therefore, it is the specific loss rate $\alpha_{\mathrm{loss},n}$ that depends in a micro-physical model on the roughness properties σ (roughness variance) and ξ (roughness correlation length), i.e., $\alpha_{\mathrm{loss},n} = \alpha_{\mathrm{loss},n}(\sigma, \xi)$. Furthermore this argument requires that micro-physical quantities should not depend on the neutron state number. Thus, we have $\alpha_{\mathrm{loss},n} = \alpha_{\mathrm{loss}},\ \forall n$. Thus, we have

$$\Gamma_n(l) = \alpha_{\mathrm{loss}} \int_{l-2\sigma}^{l} \mathrm{d}z|\psi_n(z)|^2. \tag{11}$$

We fit this quantity, α_{loss}, to the data.

This leaves us with the task to determine the integrals $\int_{l-2\sigma}^{l} \mathrm{d}z|\psi_n(z)|^2$ for a state n in a given experimental setup.

4.1 The wave guide system with gravity

The bound states $\psi_{n,g}$ in the linear gravitational potential are confined by two very high potential steps above (absorber) and below (mirror). They can be given analytically by

$$\psi_{n,g}(z) = A_n \mathrm{Ai}(z/R - \zeta_n(l)) + B_n \mathrm{Bi}(z/R - \zeta_n(l))\,, \tag{12}$$

and they fulfill the boundary conditions

$$\psi_{n,g}\big|_{z=0} = 0 \bigwedge \psi_{n,g}\big|_{z=l} = 0, \tag{13}$$

which account for the high potential steps bounding the potential from below and above. Equations (12) and (13) together determine the energy eigenvalues $\zeta_n(l)$ as functions of the absorber height l, which is done numerically.

For a given state $\psi_{n,g}$ the Ai-part in the wave function is exponentially decaying for $z > z_n(l) = \zeta_n(l)R$, while the Bi-part grows exponentially in this region. At $z = l$ both

parts add to zero. As long as $l > z_n(l)$, we have $B_n \ll A_n$ because the Bi-part has to compensate only for the exponentially small value of the Ai-part at $z = l$. This, however, implies that at $z < l$ we have $|B_n \mathrm{Bi}(z/R - \zeta_n(l))| < A_n \mathrm{Ai}(z/R - \zeta_n(l))$. Therefore, we can ignore the Bi-part of the wave function in the calculation of an asymptotic expression for the $\Gamma_{n,g}(l)$ at large l. As a result, we have

$$\psi_{n,g}(z) \approx A_n \mathrm{Ai}(z/R - \zeta_n(l)) \tag{14}$$

at $l \gg z_n$. The main effect of the Bi-part is the increase of $\zeta_n(l) > z_n$ at $l < z_n$, where the z_n are given by (6). Here we denote all quantities at $l \to \infty$ with ζ_n, A_n, etc., while the corresponding quantities of the realistic states (12) at finite l are denoted with $\zeta_n(l), A_n(l)$, etc.

The states $\psi_{n,g}$ are well approximated in the large l regime by the asymptotic WKB states

$$\psi_{n,g} \approx \frac{A_n}{2\sqrt{\pi R}} (\zeta - \zeta_n)^{-1/4} \mathrm{e}^{-\frac{2}{3}(\zeta-\zeta_n)^{3/2}}, \quad \zeta \quad > \zeta_n \,. \tag{15}$$

In the limit $l \to \infty$, we have $\zeta_n(l) \to \zeta_n$ given by (6) to 1st order in WKB and $A_n = \pi \mathrm{Bi}(-\zeta_n)$. (For $l \to \infty$ we have $\psi_{n,g}(z) = A_n \mathrm{Ai}(z/R - \zeta_n)$. Then the quoted value of A_n, which is exact, ensures that $\langle \psi_{n,g} | \psi_{n,g} \rangle = 1$.) In the case $l = R\zeta_l \lesssim z_n$, consider the WKB expression for the energy eigenvalues,

$$\int_0^{\zeta_l < \zeta_n(l)} \mathrm{d}\zeta \sqrt{\zeta_n(l) - \zeta} = \pi(n - 1/4) \,. \tag{16}$$

With

$$\int_0^{\zeta_l < \zeta_n(l)} \mathrm{d}\zeta \sqrt{\zeta_n(l) - \zeta} = \zeta_l \sqrt{\zeta_n(l)} + \mathcal{O}\left(\frac{\zeta_l^2}{\zeta_n^2(l)}\right), \tag{17}$$

we arrive at

$$\zeta_n(l) = \frac{\pi^2 (n - 1/4)^2}{\zeta_l^2} \,, \tag{18}$$

which coincides with the known box state expression for large n.

Now plugging the asymptotics of the gravitationally bound states (15) into (11), one arrives at a prediction for the loss rate that reads

$$\begin{aligned} \Gamma_{n,g}(l) &= \alpha_{\mathrm{loss}} \int_{l-2\sigma}^{l} \mathrm{d}z |\psi_{n,g}(z)|^2 \\ &\simeq \alpha_{\mathrm{loss}} \frac{\sigma}{2\pi R} |A_n|^2 \frac{\mathrm{e}^{-\frac{4}{3}\left(\frac{l - z_n}{R}\right)^{3/2}}}{\sqrt{(l - z_n)/R}}, \quad l \quad \gg z_n \,. \end{aligned} \tag{19}$$

Now look at the behavior of the total neutron flux F through the wave guide if a large number of states contribute to it (semi-classical limit). We have $F = \int_{\mathcal{A}} j_x \sim \sum_n \langle \psi_n | \psi_n \rangle$, where we get $\langle \psi_n | \psi_n \rangle$ from (8), and $\mathcal{A}$ denotes the wave guide cross section. If gravity is present, the behavior $\Gamma_{\mathrm{loss}} \sim \exp(-4/3(\zeta - \zeta_n(l))^{3/2})$ leads to the fact that, each time when $l \simeq z_n = R\zeta_n$, a new state rapidly starts to contribute to the transmission. Therefore, at a given large height l, the number of states contributing to $\phi(l)$ reads from (6)

$$l = z_n \sim N^{2/3} \Rightarrow N(l) \sim l^{3/2},$$

which yields asymptotically the classical behavior in a gravitational field. A simple phase space argument [2] shows that a perfect absorber at the top in presence of a gravitational field yields the classical transmission

$$F(l) \sim l^{3/2}. \tag{20}$$

4.2 A wave guide system without gravity

Now we can use the model to derive the loss rate for bound states in the absence of gravity. These bound states are well approximated by those which describe the quantum dynamics of a particle in a one-dimensional box with infinitely high walls, i.e. the so-called box states. They are given by

$$\psi_n = \sqrt{\frac{2}{l}} \sin\left(\frac{n\pi}{l} z\right), \tag{21}$$

which yields a loss rate given by

$$\begin{aligned} \Gamma_n(l) &= \alpha_{\mathrm{loss}} \int_{l-2\sigma}^{l} \mathrm{d}z |\psi_n(z)|^2 \\ &= \alpha_{\mathrm{loss}} \left[\frac{2\sigma}{l} - \frac{1}{2n\pi} \sin\left(\frac{4n\pi}{l}\sigma\right)\right]. \end{aligned} \tag{22}$$

A comparison of the full box state expression (second line in the above equation) with the numerical result for the loss rate with gravity, using the full states (12), is given graphically in Fig. 3.

The exact expression in the second line of (22) approaches a constant for $n \to \infty$, rendering the sum in (24) divergent. Therefore, in a realistic fit we have to include the fact that in any real experiment the number of box states N in the wave guide is finite. Firstly, the collimator system in front of the wave guide yields an input distribution for the vertical velocity of finite width. Secondly, for wider vertical velocity spectra, all neutrons with $v_z > v_z^{\mathrm{crit}} = 4.3\,\mathrm{m\,s^{-1}}$, the critical velocity of glass, will enter the mirror or the absorber directly without forming bound states in the wave guide. In both cases, the number of box states populated by the entering flux of neutrons behaves like $N \sim l$. If the collimator is tuned to yield an input distribution for the vertical velocity of small width (i.e. about 10 cm/s) we have $N/l \sim 2\,\mu\mathrm{m}^{-1}$, corresponding to about $N \approx 200$ box states in a wave guide of $l \sim 100\,\mu$m width. Thus, we have evaluated a finite sum with $N/l = 2\,\mu\mathrm{m}^{-1}$ when comparing the gravity-free prediction of (24) with the experimental data sets (for $l < 100\,\mu$m, we have $N < 200$ box states populated with N approaching ≈ 200 for $l \to 100\,\mu$m). The dependence of our result on the

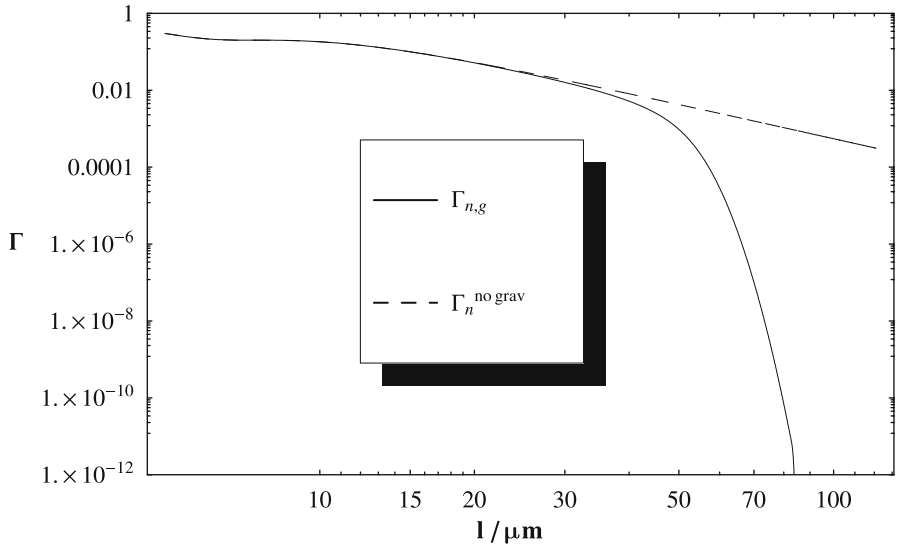

Fig. 3. Behavior of the loss rate Γ (plotted in arbitrary units) for the pure box state $n = 5$ (*dash*), an approximate power law, and for the gravitationally bound state $n = 5$ found numerically from using the full states (12) (*solid*), showing exponentially fast decay above some $l = \mathcal{O}(R)$

choice of the cutoff N is very weak. If the critical velocity of glass defines the cutoff, this results in $N/l \sim 20\,\mu\mathrm{m}^{-1}$ (corresponding to about $N \approx 2 \times 10^3$ box states in a wave guide of $l \sim 100\,\mu$m width). We find that the predictions agree for both cutoff choices with each other far better than to the experimental accuracy within the l-range of the measurement.

Now in the absence of gravity the asymptotic behavior of the transmitted flux $F(l)$ carried by the box states at large l can be given directly from (8) and (22). For $n\sigma/l \ll 1$, we can approximate (22) with

$$\Gamma_n(l) = \alpha_{\mathrm{loss}} 16\pi^2/3\sigma^3 \frac{n^2}{l^3}\,, \quad \frac{n\sigma}{l} \ll 1\,. \tag{23}$$

If the approximation in (23) were valid for all n, we would have

$$\begin{aligned} F(l) &\sim \sum_{n\geq 1} \mathrm{e}^{-\Gamma_n(l) t_{\mathrm{flight}}} \\ &= \sum_{n\geq 1} \mathrm{e}^{-\gamma n^2} \\ &= \frac{1}{2}(\vartheta_3(0, \mathrm{e}^{-\gamma}) - 1) \\ &\sim l^{3/2}\,, \quad \text{for large } l. \end{aligned} \tag{24}$$

Here $\gamma = 16\pi^2/3\sigma^3 l^{-3} t_{\mathrm{flight}}$ and $\vartheta_n(q, u)$ denotes the elliptic theta function, where we used *Mathematica* [22] to evaluate the sum. This result differs from the naive classical behavior of a gravity-free wave guide with a perfect absorber: in the case of the linear trajectories describing classical particles in the absence of the gravitational field, we find [19]

$$F(l) \sim l^2, \tag{25}$$

which is easy to imagine, since one factor of l obviously has its origin in the relation $F(l) \sim \mathcal{A} \sim l$, while the second factor encodes that the range of vertical velocities Δv_z of particles that pass the wave guide without ever touching the absorber also behaves like $\Delta v_z \sim l$.

Finally, from this situation we expect in general an interpolating behavior of the gravity-free transmission rate with respect to its power-law dependence on the absorber height. In fact, if the gravity-free prediction of (24) is carried out using the exact expression for the loss rates Γ_n in (22) for $N/l > 200\,\mu\mathrm{m}^{-1}$, i.e. $N > 2 \times 10^4$ box states at $l \approx 100\,\mu$m, we find that the transmission begins to deviate from an $l^{3/2}$-power law towards an l^n-dependence with $n \to 2$, which is the general dependence to be expected both classically and quantum mechanically. Thus, the behavior of the gravity-free prediction as $F(l) \sim l^{3/2}$ in our given experimental situation is an artifact caused by the relatively small number of box states ($N \lesssim 2 \times 10^3$ for $l \leq 100\,\mu$m) in the wave guide.

4.3 Reversed geometry

We now turn to the third case, of $g \to -g$ instead of $g \to 0$. This inversion of gravity is equivalent to a setup geometry in which the absorber/scatterer is placed at the bottom at $z = 0$ and a movable mirror at $z = l$ above the absorber. For this situation we can follow the derivation of Sect. 4.1. Since the absorber is now at $z = 0$, we have to evaluate the probability integral at this position, which implies for large l the use of the asymptotic WKB expression

$$\begin{aligned} &\psi_{n,g} \approx \frac{A_n}{\sqrt{\pi R}} (\zeta_n - \zeta)^{-1/4} \sin\left[\frac{2}{3}(\zeta_n - \zeta)^{3/2} + \frac{\pi}{4}\right], \\ &\zeta < \zeta_n\,. \end{aligned} \tag{26}$$

This results in

$$\Gamma_{\mathrm{loss}}^{(n,g,\mathrm{rev.})}(l) = \alpha_{\mathrm{loss}} \frac{\sigma}{2\pi R} |A_n|^2 \frac{16}{3} \sqrt{\frac{z_n}{R}} \frac{\sigma^2}{R^2}\,. \tag{27}$$

Note that this loss rate of the reversed geometry is practically independent on the state number n, since

$\lim_{n\to\infty}|A_n|^2\sqrt{\zeta_n}=\pi$, and even at $n=1$ it is $|A_1|^2\sqrt{\zeta_1}/\pi-1\lesssim 0.5\%$. Comparing this result with the corresponding expression (19) for the normal geometry, we find that the ratio of the fluxes $F_n^{(\mathrm{g}),\mathrm{rev.}}(l)/F_n^{(\mathrm{g})}(l)$ of the nth state for $l>z_n$ between the reversed and the normal geometry is given by

$$\frac{F_n^{(\mathrm{g}),\mathrm{rev.}}(l)}{F_n^{(\mathrm{g})}(l)}=\mathrm{e}^{-\alpha_{\mathrm{loss}}\frac{\sigma}{2\pi R}|A_n|^2\frac{16}{3}\sqrt{\frac{z_n}{R}}\frac{\sigma^2}{R^2}\frac{L}{v_{\mathrm{hor.}}}}. \tag{28}$$

Since $\frac{\sigma}{2\pi R}|A_1|^2\frac{16}{3}\sqrt{\frac{z_1}{R}}\frac{\sigma^2}{R^2}\frac{L}{v_{\mathrm{hor.}}}\approx 7.2\times10^{-5}\,\mathrm{s}$ for the experimental values of $L=0.13\,\mathrm{m}$, $v_{\mathrm{hor.}}\approx 10\,\mathrm{m/s}$ and $\sigma=0.75\,\mu\mathrm{m}$, a value of $\alpha_{\mathrm{loss}}\gtrsim\mathcal{O}(10^4\,\mathrm{s}^{-1})$ fitted from a measurement of the normal geometry would result in a huge asymmetry under a π-rotation around the optical axis of the wave guide when comparing the normal and the reversed geometry.

5 A fit to the data

For a comparison with the measurements we plug the resulting loss rates into the general prediction for the transmitted neutron flux (29). Together with the repopulation coefficient p_1 accounting for eventual shifts between split bottom mirrors, one predicts

$$\begin{aligned}F(l)&=F_0+\sum_n F_n(l)\\&=F_0+C\left\{p_1\mathrm{e}^{-\Gamma^{(1)}_{\mathrm{loss}}(l)\frac{L}{v_{\mathrm{hor.}}}}+\sum_{n>1}\mathrm{e}^{-\Gamma^{(n)}_{\mathrm{loss}}(l)\frac{L}{v_{\mathrm{hor.}}}}\right\}.\end{aligned} \tag{29}$$

F_0 is the detector background and C the total flux normalization. α_{loss} is the universal parameter introduced above, which parameterizes the scatterer strength. This quantity is in general expected to be a rather weak function of the roughness parameters σ and ξ that would be determined in principle by a micro-physical calculation of the loss due to non-specular scattering at the rough absorber surface. Thus, it does not depend on the absence or presence of gravity nor on the state number n.

In the case of $l\lesssim z_n$, the absorber/scatterer will begin to squeeze the bound states once they start to 'feel' it sufficiently strongly. This implies further that due to $E_{n,g}(l)\geq E_{n,g}(\infty)=E_{n,g,\mathrm{pure\ gravity}}$ for the true bound states, a sufficiently small l leads to $E_{n,g}(l)\gg mgl$. Therefore, the calculation of the $\Gamma^{(n)}_{\mathrm{loss}}$ is done using the full realistic bound states (12) and deriving the relations corresponding to (19), (22) and (27) numerically, which incorporates the mentioned behavior.

5.1 Normal geometry

The detector background ϕ_0 has been measured independently to yield $F_0=(0.0043\pm0.0004)\,\mathrm{s}^{-1}$ for the 1999 measurement [1] and $F_0=(0.0004\pm0.0001)\,\mathrm{s}^{-1}$ for the new 2002 measurement using an improved setup [20]. Thus, one finds oneself having to determine the two universal quantities α_{loss} and C from the data. C turns out to be completely fixed by the data points at $l>70\,\mu\mathrm{m}$ and thus also has been measured. The fit therefore will be a 1-parameter one, determining α_{loss} as long as all the populations p_n stay equal.

We fit now (29) to the newer data from the run of the experiment in 2002, which has a different absorber and better statistics, and the systematic effects are smaller than in 1999. The results are shown in Fig. 2. The value of α_{loss} is found in a fit to the data. The result of the fit yields ($L=13\,\mathrm{cm}$, $v_{\mathrm{hor.}}\approx 5\,\mathrm{m\,s}^{-1}$)

$$\alpha_{\mathrm{loss}}=(3.4\pm0.1)\times10^4\,\mathrm{s}^{-1}. \tag{30}$$

The fit was done using neutrons with only one value of the horizontal velocity, which was chosen to be the average velocity $v_{\mathrm{hor.}}\approx 5\,\mathrm{m\,s}^{-1}$. This approximation produces essentially the same results as if one uses the full actual spectrum of horizontal velocities produced by the collimating system to calculate the transmission.

The 2002 run was performed with only one bottom mirror, so that no significant repopulation effects of the ground state are expected. However, it was necessary to allow the population of the ground state to shift towards 75% compared to the excited states in order to describe the data: $p_1=0.77\pm0.04$. This suppression is significant, but it is not large, leaving all the states still to be approximately equally populated.

In the measurement of the 1999 run, two bottom mirrors were used. One tried to shift these mirrors relative to each other vertically and in alignment by a few micrometers. Small shifts of a few microns between the two bottom mirrors change the population of the ground state and the next state quite drastically: a shifted geometry with a relative mirror shift of about $5\,\mu\mathrm{m}$ and no relative tilt of the two bottom mirrors results in $p_1\approx 0.25$, to be compared to $p_n=1$, $n\geq 2$. The fit to the data (see Fig. 4) results in $\alpha_{\mathrm{loss}}=(5.3\pm0.5)\times10^4\,\mathrm{s}^{-1}$ and $p_1=0.24\pm0.1$, which would be consistent with the possible relative mirror shift discussed above.

5.2 Reversed geometry

In a second setup described by the term 'reversed geometry', the absorber was placed at the bottom and the mirror above. Here, the position of the scattering-inducing roughness is found at $z=0$. This case can also be derived from the states (12) by just placing the roughness appropriately on the bottom and then calculating the corresponding loss rates. The bound states are now again given by the Airy functions. However, at $z=0$, where the absorber is now placed, they do not decay exponentially fast, and the gravitationally bound states will be strongly absorbed at arbitrary heights l of the mirror at the top – quite contrary to the normal setup. If gravity were absent, such a π-turn of the wave guide around its optical axis would not have such an effect. Thus, there would be

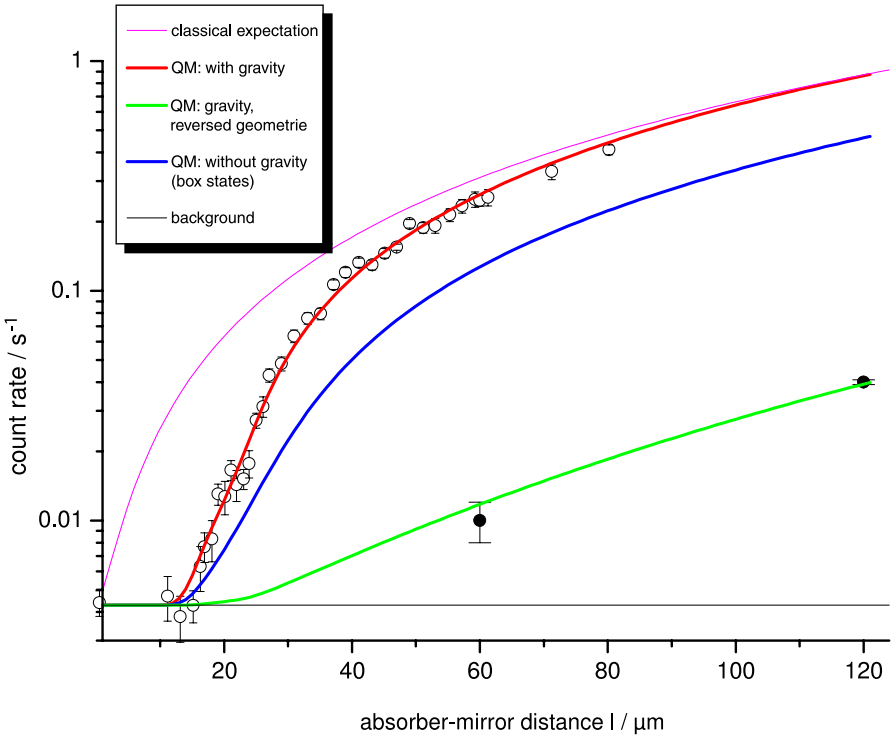

Fig. 4. *Open circles*: transmission as a function of the absorber–mirror distance. *Filled circles*: transmission measured with inverse geometry – the absorber on the bottom and a 10 cm mirror on top (both are 1999 measurement data [2])

no preferred direction in space forcing the transmission factor to be invariant under rotations around the optical axis of the system, since the box states describing the simple confinement situation without gravity are symmetric with respect to the optical axis. This check was done with the 1999 data. We took the prediction for gravitationally bound states of (12) in the normal setup and fitted α_{loss} and p_1 to the data. The model yields $p_1 = 0.24 \pm 0.1$ and $\alpha_{\mathrm{loss}} = (5.3 \pm 0.5) \times 10^4\,\mathrm{s}^{-1}$. Taking now these values for α_{loss} and p_1 from the fit, we can calculate a prediction for the setup with reversed geometry using the results of Sect. 4.3 – which is now entirely fixed and not fitted any more. Using the experimental setup parameters used there, $L = 13\,\mathrm{cm}$ and $v_{\mathrm{hor.}} \approx 10\,\mathrm{m/s}$, we can estimate the suppression factor using (28) on the ground state, which yields

$$\frac{F_1^{(\mathrm{g}),\mathrm{rev.}}(l)}{F_1^{(\mathrm{g})}(l)} \approx 0.03\,. \tag{31}$$

This fits well with the two data points obtained experimentally in this reversed setup. Using the full prediction calculated again numerically from (12) in the reversed setup, the comparison with the 1999 data is shown in Fig. 4. In treating the 1999 data, other models [2, 11] showed more pronounced steps. These steps are not present in the (more advanced) model presented in this paper.

The above described asymmetry of the neutron transmission of a wave guide with one absorbing and one reflecting wall under rotations around its optical axis in the presence of gravity has indeed been measured and can be described quantitatively. This rules out the possibility to explain the data just by confinement effects in terms of box states inside a rectangular box-shaped potential [23], and thus it establishes the gravitational nature of the force that binds the neutron bound states to the bottom mirror. For further discussion, see also [24]. The measurement of the reverse geometry is a very good test of our (or probably any) model, since the result depends strongly on the absorber properties. The fact that the absorber model that describes the data in the normal geometry can also be used for the reversed geometry, without any new fit parameters, gives us confidence that our model is a useful tool for describing the data.

6 Summary

For the first time the existence of quantized bound states of neutrons in the gravitational field of the earth above a horizontal glass mirror was experimentally demonstrated. Here we present a quantum mechanical model providing an accurate fit to the data. The difficult part is the incorporation of the neutron absorber into this model. We show that we can describe its action with only one phenomenological fit parameter in several configurations. The most important configuration has bound quantum states in the linear gravitational potential. We consider repopulation effects of these states when a step from a second mirror is present. The emerging reduction of the first state has been calculated. The standard setup uses only one mirror. Also in this case, the data show an unexpected reduction of the first quantum state as well.

Further, it is shown that the experiment would generate different results if gravity were hypothetically to be turned off. This configuration is a wave guide system

with box states that describe the quantized motion of a particle in a one-dimensional box with infinitely high walls.

A striking difference is found, if the gravitational field changes sign. This case has been observed by putting the mirror and absorber upside down in our measurement [1] and can be described quantitatively within the same modeling of the absorber mechanism presented here. Thus, the dominating effect of gravity on the formation of the bound states has been demonstrated, since the measurement did not show just a simple confinement effect, as proposed in [23]. On the contrary, the data cannot be described if the earth's gravitational field was not present.

References

1. V.V. Nesvizhevsky et al., Nature **415**, 297 (2002)
2. V.V. Nesvizhevsky et al., Phys. Rev. D **67**, 102 002 (2003) [hep-ph/0306198]
3. V.I. Luschikov, A.I. Frank, JETP Lett. **28**, 559 (1978)
4. V.V. Nesvizhevsky et al., Nucl. Instrum. Methods A **440**, 754 (2000)
5. H. Wallis et al., Appl. Phys. B **54**, 407 (1992)
6. R.L. Gibbs, Am. J. Phys. **43**, 25 (1975)
7. H.C. Rosu, quant-ph/0104003
8. C.G. Aminoff et al., Phys. Rev. Lett. **71**, 3083 (1993)
9. M.A. Kasevich, D.S. Weiss, S. Chu, Opt. Commun. **15**, 607 (1990)
10. T.M. Roach et al., Phys. Rev. Lett. **75**, 629 (1995)
11. H. Abele, S. Baeßler, A. Westphal, Lect. Notes Phys. **631**, 355 (2003) [hep-ph/0301145]
12. V.V. Nesvizhevsky, K.V. Protasov, Class. Quantum Grav. **21**, 4557 (2004) [hep-ph/0401179]
13. N. Arkani-Hamed, S. Dimopoulos, G.R. Dvali, Phys. Lett. B **429**, 263 (1998) [hep-ph/9803315]
14. I. Antoniadis, N. Arkani-Hamed, S. Dimopoulos, G.R. Dvali, Phys. Lett. B **436**, 257 (1998) [hep-ph/9804398]
15. N. Arkani-Hamed, S. Dimopoulos, G.R. Dvali, Phys. Rev. D **59**, 086 004 (1999) [hep-ph/9807344]
16. I. Antoniadis, Lect. Notes Phys. **631**, 337 (2003)
17. D. Cremades, L.E. Ibanez, F. Marchesano, Nucl. Phys. B **643**, 93 (2002) [hep-th/0205074]
18. C. Kokorelis, Nucl. Phys. B **677**, 115 (2004) [hep-th/0207234]
19. A. Westphal, Diploma thesis (Institute of Physics, University of Heidelberg, 2001) [gr-qc/0208062]
20. V.V. Nesvizhevsky et al., Eur. Phys. J. C **40**, 479 (2005) [hep-ph/0502081]
21. A.Y. Voronin et al., quant-ph/0512129
22. S. Wolfram, The Mathematica Book, 4th edn. (Cambridge University Press, Cambridge, 1999)
23. J. Hansson, D. Olevik, C. Turk, H. Wiklund, Phys. Rev. D **68**, 108 701 (2003) [quant-ph/0308108]
24. V.V. Nesvizhevsky et al., Phys. Rev. D **68**, 108 702 (2003)